Current Biology 20, 513–520, March 23, 2010 ©2010 Elsevier Ltd All rights reserved DOI 10.1016/j.cub.2010.01.063

Report

Dpp Signaling Directs Cell Motility and Invasiveness during Epithelial Morphogenesis

Nikolay Ninov,[1,5,6] Sofia Menezes-Cabral,[1,2,5] Carla Prat-Rojo,[1] Cristina Manjón,[1] Alexander Weiss,[3] George Pyrowolakis,[3,4] Markus Affolter,[3] and Enrique Martín-Blanco[1,*]

[1]Instituto de Biología Molecular de Barcelona, Consejo Superior de Investigaciones Científicas, Parc Científic de Barcelona, Baldiri Reixac 10, 08028 Barcelona, Spain
[2]Programa Doutoral em Biologia Experimental e Biomedicina, Center for Neuroscience and Cell Biology, University of Coimbra, 3004-517 Coimbra, Portugal
[3]Abteilung Zellbiologie, Biozentrum der Universität Basel, Klingelbergstrasse 70, CH-4056 Basel, Switzerland
[4]Institute of Biology I, University of Freiburg, Hauptstraße 1, D-79104 Freiburg, Germany

Summary

Tissue remodeling in development and disease [1, 2] involves the coordinated invasion of neighboring territories and/or the replacement of entire cell populations. Cell guidance, cell matching, transitions from passive to migratory epithelia, cell growth and death, and extracellular matrix remodeling all impinge on epithelial spreading. Significantly, the extracellular signals that direct these activities and the specific cellular elements and mechanisms regulated by these signals remain in most cases to be identified. To address these issues, we performed an analysis of histoblasts (*Drosophila* abdominal epithelial founder cells [3, 4]) on their transition from a dormant state to active migration replacing obsolete larval epidermal cells (LECs). We found that during expansion, Decapentaplegic (Dpp) secreted from surrounding LECs leads to graded pathway activation in cells at the periphery of histoblast nests. Across nests, Dpp activity confers differential cellular behavior and motility by modulating cell-cell contacts, the organization and activity of the cytoskeleton, and histoblast attachment to the substrate. Furthermore, Dpp also prevents the premature death of LECs, allowing the coordination of histoblast expansion to LEC delamination. Dpp signaling activity directing histoblast spreading and invasiveness mimics transforming growth factor-β and bone morphogenetic proteins' role in enhancing the motility and invasiveness of cancer cells, resulting in the promotion of metastasis [5, 6].

Results

Histoblast Nest Expansion

Drosophila histoblasts are born as small groups of cells specified during embryogenesis that organize as polarized monolayer epithelium patches (histoblast nests). They are embedded in the abdominal larval epidermis and proliferate and expand during metamorphosis to replace the larval epithelial cells (LECs). We have found that histoblasts at the periphery of the nests flatten and move in between LECs, pushing them apart [4] (Figures 1A and 1B; see also Movie S1 available online). Furthermore, the area occupied by the histoblast nests during the expansion phase increases faster than the number of cells, and mostly at the periphery (see Figure 1C). The number of cells does not increase at a sufficient rate to compensate for the increase in nest area, and histoblasts become stretched in different directions and flatten as the nest periphery expands while invading the LEC landscape. Thus, nests' spreading is mostly a consequence of cell surface growth. We have also observed that blocking LEC death prevents nest expansion and peripheral histoblast flattening [4]. However, this did not suppress histoblast proliferation or invasive activity at the periphery (Movie S2). Together, these data suggest that for abdominal epithelial replacement, histoblast proliferation [7] and LEC extrusion, which facilitates histoblast nest expansion by "getting LECs out of the way" [4], are coupled to the invasive activity of leading histoblasts at the nest periphery.

At the onset of expansion, three key cellular changes took place in the peripheral histoblasts. First, their actin cytoskeleton became highly dynamic and they showed extremely active, both apical and basal, filopodia and lamellipodia (Movie S3A). They also extended long, thick actin-rich protrusions, which intercalated within adjacent LECs [4] (Figure 1D; see also Figure S1F). All of the hallmarks of leading histoblast motility—filopodia, lamellipodia, long terminal extensions, and their invasive capability—are abolished upon interference with actin dynamics [4]. Second, as expansion proceeded, histoblasts at the periphery gradually reduced the density of adherens junction (AJ) and septate junction (SJ) components (Figure 1E and data not shown). These observations correlate with the weakening of cell-cell contacts between histoblasts at the nest periphery visualized in 3D reconstructions of confocal images (Movie S3B). Finally, β-integrin expression in leading histoblasts was only found in apical spots, whereas it was mostly basolateral in the center of nests (Figure 1F). This relocation of β-integrin was temporally associated with the degradation of the basal lamina from 16 hr after puparium formation (APF) onward (Figures S1A and S1B). The absence of extracellular matrix (ECM) and the loss of basal integrins suggest that leading histoblasts may not use a basal support as a substrate for migration. In this scenario, apical integrins might mediate histoblast apical crawling. To evaluate this possibility, we performed ultrastructural analyses, which revealed that leading histoblasts are tightly attached apically to the overlaying chitin layer, as would be expected if they used the pupal cuticle as spreading substrate (compare Figures S1D and S1G to Figure S1E). In addition, we found conspicuous apical filopodia and lamellipodia at the front of leading histoblasts as they spread forward (see Movie S3C).

These observations together show that histoblast invasiveness is linked in the leading cells to changes in actin dynamics and remodeling of cell-cell contacts and cell-substrate adhesion.

*Correspondence: embbmc@ibmb.csic.es
[5]These authors contributed equally to this work
[6]Present address: Department of Biochemistry & Biophysics, University of California, San Francisco, San Francisco, CA 94158, USA

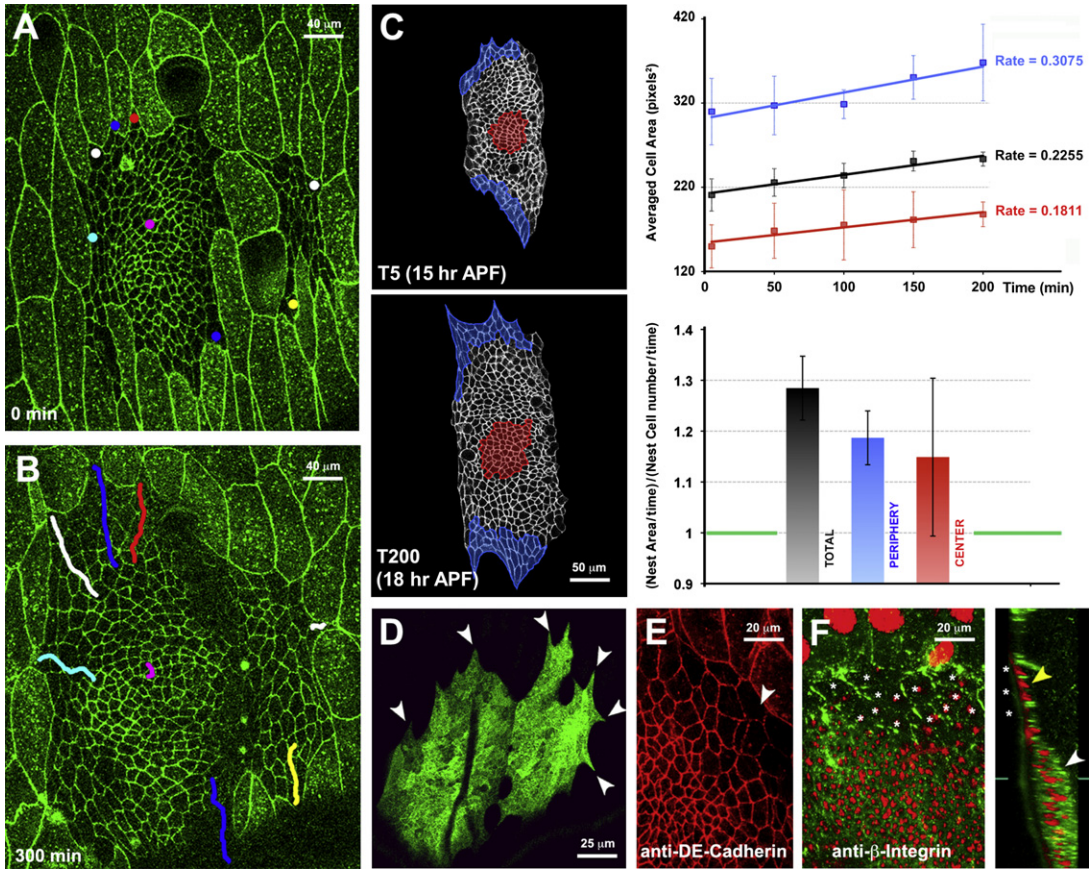

Figure 1. Histoblast Invasion of Larval Territories Is Carried Out by Peripheral Histoblasts, which Undergo Changes in Actin Dynamics and in Cell-Cell and Cell-Matrix Adhesion

(A and B) Wild-type anterior and posterior dorsal nests and larval epidermal cells (LECs) at 17–18 and 22–23 hr after puparium formation (APF) expressing DE-cadherin-GFP (green) (from Movie S1). At these stages, histoblasts invade the larval epidermis by planar intercalation. Cells at the periphery of the nests become active and penetrate between adjacent LECs, leading to nest expansion and fusion. In contrast, cells in the center of the nests remain passive and maintain constant relative positions and shapes. Colored lines and dots represent the tracking and relative displacement of peripheral and central histoblasts between these two time points.

(C) The area and the number of cells of individual anterior dorsal histoblast nests (n = 3) were examined between ~15 and ~18 hr APF. Area and cell numbers were quantified for the whole nests (443–482 cells per nest at T0 [~15 hr APF]) and selected regions (expanding periphery, 39–45 cells per nest at T0, blue; center, 42–50 cells per nest at T0, red). Upper right: averaged individual cell areas (and standard deviations) were plotted versus time for all (black), central (red), and peripheral (blue) histoblasts. These measurements showed that individual cell areas increased linearly and at a faster rate at the periphery. Lower right: histograms showing the ratio of the rate of nest area increase to rate of cell number increase (± standard deviation). The green line highlights a ratio of 1, which would correspond to equivalent growth rates for nest area and cell numbers. Total nest, periphery, and central region area growth rates are in all cases higher than the corresponding rate of cell number increase (rate ratios = 1.28 [total], 1.18 [periphery], and 1.15 [center]). These calculations show that the spreading of the nests is primarily caused by an active expansion of the tissue (mainly at the periphery) and cannot be attributed merely to cell proliferation.

(D) Wild-type anterior and posterior dorsal nests labeled in vivo by actin-GFP (green) driven by the *esg*-Gal4 driver. Cells at the periphery extend long invasive protrusions.

(E) During expansion of the nests, DE-cadherin (red) density is lowered in flattened histoblasts at the periphery of the nest (arrowhead). DE-cadherin levels (total accumulated pixel signal intensity per cell) were equal for all histoblasts (1594.29 ± 101.75 arbitrary integrated density [ID] units per cell). However, DE-cadherin density at the cell membrane (ratio of accumulated pixel signal intensity at the membrane to cell perimeter) was significantly reduced ($p = 0.01$) in histoblasts at the periphery versus those at the center (6.61 ± 0.54 versus 10.38 ± 0.80 ID units per perimeter unit, respectively) (n = 11 from four different individuals for each condition).

(F) Peripheral histoblasts (asterisks) lack β-integrin localization (green) at their basal surface (yellow arrowhead), whereas centrally located cells show abundant β-integrin on matrix attachments (white arrowhead). Nuclei are marked in red with DAPI. See also Figure S1 and Movies S1–S3.

Dpp Signaling Is Necessary for Histoblast Expansion

The change in histoblast behavior at the onset of spreading indicates that the triggering and maintenance of motility and invasiveness are induced by specific temporally and spatially controlled signals. To test the involvement of discrete signaling modules in instructing histoblast invasiveness, we evaluated the ability of cells mutant for key signaling elements to lead histoblast nest spreading in mosaics. We analyzed clones homozygous mutant for receptors or downstream effectors for epidermal growth factor (EGF), insulin/phosphatidylinositol 3-kinase (PI3K), fibroblast growth factor (FGF), Hedgehog (Hg), Wingless (Wg), Decapentaplegic (Dpp), Jun N-terminal kinase (JNK), and platelet-derived vascular endothelial growth factor (PVF) signaling (see Supplemental Experimental Procedures). Wild-type cell clones were found to be compact and had a tendency to elongate along the dorsoventral axis, and

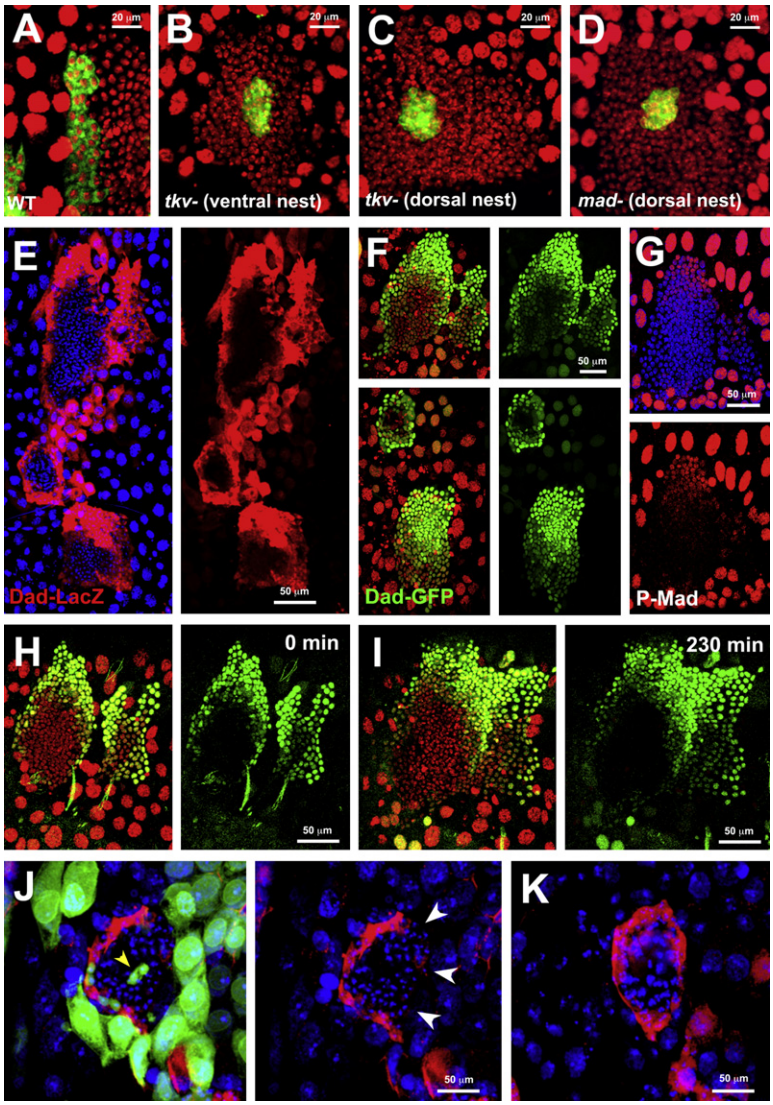

Figure 2. Dpp Signaling Is Activated in Histoblasts and Larval Epidermal Cells, and Interference with Dpp Signaling Abolishes Histoblast Invasiveness

(A) A wild-type mosaic analysis with a repressible cell marker (MARCM) clone (green) at 22 hr APF induced in the anterior dorsal nest. This clone shows characteristic dorsoventral elongation and contributes to the nest leading edge.

(B and C) Clones homozygous mutant for the Dpp receptor *tkv* at 22 hr APF in ventral (B) and anterior dorsal (C) nests. These clones display a condensed round shape, do not contribute to the expanding periphery, and remain in the nest center.

(D) Clones of *mad* show a phenotype identical to *tkv* (dorsal nest at 22 hr APF).

(E) *dad*-LacZ reporter (red) specifically labels the cells at the periphery of each histoblast nest (18–19 hr APF).

(F) *dad*-GFP reporter (green) also labels the cells at the periphery (18–19 hr APF). His2-RFP (red) labels all nuclei.

(G) p-Mad staining highlights the histoblasts at the periphery of dorsal anterior and posterior nests with a similar pattern (20–23 hr APF). Remarkably, p-Mad also marks *dpp*-expressing LECs.

(H and I) Time-lapse in vivo study of Dpp activity during histoblast expansion with His2-RFP (red) to label all nuclei and *dad*-GFP (green). Snapshots taken from Movie S4A show that the expansion of the dorsal anterior and posterior nests initiates at 18–19 hr APF. From this time onward, cells exhibiting higher levels of Dpp signaling are found at the nest periphery clustering at invading puncta (see Movie S4B).

(J) Clonal expression of a Dpp RNAi construct (GFP-labeled cells) in LECs and histoblasts (yellow arrowhead). The Dpp RNAi expression in LECs results in downregulation of Dpp activity (monitored by the expression of a *dad*-LacZ reporter, red) in adjacent histoblasts (white arrowheads). The figure depicts a spiracular histoblast nest at 17 hr APF.

(K) Control wild-type spiracular histoblast nest at 17 hr APF showing Dpp signaling activity (*dad*-LacZ reporter, red) at the entire periphery.

Nuclei are marked in red in (A)–(D) and in blue in (E), (G), (J), and (K) with DAPI. See also Figure S2 and Movie S4.

by 22–26 hr APF, 60% of them on average (n = 43) contributed to the nest periphery (Figure 2A). In sharp contrast, the proportion of clones mutant for *tkv* (which encodes the Dpp type I receptor Thick veins) or for *mad* (which encodes a transcriptional effector of the Dpp pathway [8]) abutting the nest edge was markedly reduced to 20% (n = 36 and n = 22) (Figures 2B–2D). Importantly, the histoblasts unable to respond to Dpp proliferated at normal rates and did not delaminate or die (see below). In summary, histoblasts not responding to Dpp remained naive and did not invade neighboring territories. These phenotypes were not observed for any other signaling pathway (data not shown).

Dpp Is Activated in Histoblasts and LECs at the Onset of Histoblast Spreading: Paracrine and Autocrine Functions

dpp initiated its expression in dorsal and ventral nests in a discrete dorsal anterior domain (Figures S2A and S2C). This pattern, in agreement with previous reports [9], evolved through metamorphosis to delineate the anterior-posterior compartment border. In addition to its expression in histoblasts, *dpp* was also expressed in all LECs surrounding each nest from the midpupal transition onward (Figures S2B and S2D).

Dpp signaling in histoblasts immediately adjacent to LECs (but not in those more central) was switched on at a time coincident with the onset of *dpp* LEC expression and nest expansion. Using a LacZ enhancer trap inserted in *dad* (a direct transcriptional target of Dpp), we found that the transcriptional response to the pathway was specifically activated in histoblasts at the nest periphery and a few LECs (Figure 2E). We further monitored Dpp activity in live transgenic flies with a fluorescent Dpp signaling sensor built by fusing a conserved minimal *dad* enhancer [10] to a nuclear GFP reporter (see Supplemental Experimental Procedures). Again, the *dad*-GFP reporter highlighted those cells at the periphery of the nest first engaged in directional motility and planar intercalation (Figures 2F, 2H, and 2I; Movies S4A and S4B). Strikingly, we found that the activation of Dpp signaling (*dad*-LacZ reporter) in leading histoblasts was abolished by interfering with Dpp expression in LECs clonally expressing a Dpp RNA interference (RNAi) construct (Figures 2J and 2K). Together, these findings suggest a transcriptionally enforced paracrine instrumental role for Dpp in histoblasts supporting motility and invasiveness at the nest periphery.

To test the potential paracrine role of Dpp, we clonally expressed the Dpp signaling inhibitor Dad in combination

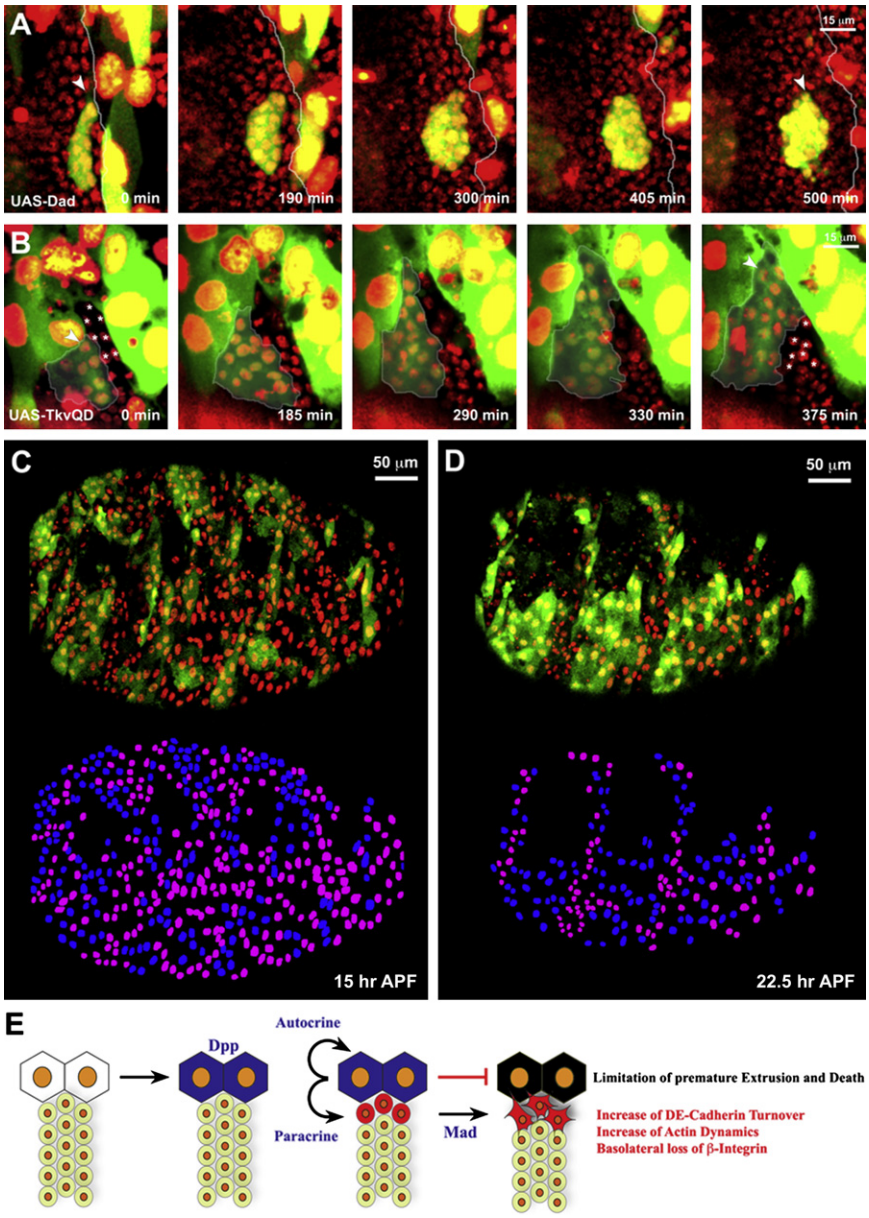

Figure 3. Paracrine and Autocrine Functions of Dpp

(A) Time-lapse analysis of a clone overexpressing UAS-Dad labeled with GFP (green) in the dorsal edge of the anterior dorsal nest (from Movie S5A). Clones were induced via the FLP-OUT/FRT system. Nuclei were labeled with His2-YFP (red). At 0 min (15 hr APF), Dad-overexpressing cells show normal cell morphology and contact the nest edge (arrowhead). At 190 min, the expansion of histoblasts has initiated and the clone loses contact with the edge. At 300 min, the clone is completely excluded from the edge and surrounded by wild-type cells. At 405 min, the clone shows condensed and rounded cell morphology similar to *tkv* or *mad* clones. The white line delineates the nest edge.

(B) Time-lapse analysis of a Tkv^{QD} clone (arrowhead) in the posterior dorsal nest (Movie S5B) reveals enhanced cell motility. At 0 min (16 hr APF), the clone shares the edge with wild-type cells (asterisks). At 185 min, the nest initiates expansion in dorsal directions. At 290 min, the Tkv^{QD} cells begin to colonize the expanding tip. At 375 min, the tip is composed entirely of Tkv^{QD}-expressing cells. Wild-type cells initially in contact with the edge lag behind (asterisks). In all panels, the large polyploid nuclei correspond to LECs. A translucent mask defines the periphery of the clone. Nuclei were labeled in red with His2-YFP.

(C and D) Mosaic clonal overexpression of Tkv^{QD} in LECs results in a reduction of their delamination rate. LECs overexpressing Tkv^{QD} were marked with GFP, and their extrusion from the epithelia (and that of neighboring wild-type [WT] LECs) was monitored from 15 to 22.5 hr APF. Nuclei of all cells were labeled by His2-YFP (red) expression. Tkv^{QD}-expressing (blue) and WT sibling (pink) LEC nuclei were identified and counted at different time points (lower panels). Those LEC nuclei that became lost from the field during the 7.5 hr observation period were discarded from the analysis. The rate of delamination was calculated as the percentage of LECs that extruded per hour. Tkv^{QD} LECs delaminated at a rate of 2.6% cells per hour, whereas WT LECs delaminated at a rate of 7% cells per hour.

(E) A mechanistic model for Dpp signaling. *dpp* expression is activated in LECs at the onset of histoblast spreading, leading to paracrine (in histoblasts) and autocrine (in LECs) activation of Dpp signaling. In histoblasts, this activity, executed at the transcriptional level by Mad, leads to a complex, multifaceted phenotype. At the cellular level (see Figure 4), Dpp signaling results in an increase of DE-cadherin turnover at the membrane, reduction of DE-cadherin density in leading histoblasts, and a relaxation of cell-cell contacts. Furthermore, Dpp signaling enhances actin microfilament dynamics and modulates the subcellular localization of integrins. On the other hand, autocrine Dpp signaling in LECs appears to prevent their precocious delamination. See also Figure S3 and Movie S4.

with a general nuclear YFP marker in histoblasts and followed the behavior of mutant cells by time-lapse microscopy. We found that prior to the onset of epithelial expansion, Dad-expressing cells could form part of the periphery of the nests and displayed normal shape and size. Upon initiation of spreading, however, Dad-expressing clones became highly condensed and were quickly excluded from the periphery (Figure 3A; Movie S5A). To test whether Dpp signaling activation can autonomously promote histoblast invasiveness, we analyzed the motility of histoblasts under hyperactive Dpp signaling conditions. Clonal overexpression of a constitutively active Dpp receptor (Tkv^{QD}) in histoblasts resulted in increased predisposition to associate with the periphery, with 75% of the clones contacting the nest edges (n = 40). Histoblasts underwent dramatic morphogenetic changes, became extremely motile, and progressively replaced wild-type cells at the periphery. occupying leading positions (Figure 3B; Movie S5B). As described above for *tkv* and *mad* clones, neither Tkv^{QD} nor Dad overexpression affected histoblast proliferation (Figure S3 and data not shown). In summary, the relative strength of Dpp signaling activation dictates the degree of cell motility and plasticity of histoblasts during the invasion of the larval epidermis.

Remarkably, following the upregulation of *dpp* expression detected in LECs (Figures S2C and S2D), we observed that antibodies against phosphorylated Mad (p-Mad) showed

a strong signal in LECs, along with expression in peripheral histoblasts, from 16 hr APF onward (Figure 2G). Thus, Dpp signaling may be playing an autocrine role in LECs independent of Mad-mediated transcriptional activation of *dad* expression (see Figures 2J and 2K). This function may lead to adhesive and cytoskeletal differences between LEC neighbors affecting cell extrusion. To analyze this possibility, we studied LECs clonally overexpressing Tkv^{QD} and found that hyperactivating the pathway resulted in the slowing of LEC delamination from 7.0% ± 1.4% (wild-type [WT] siblings) to 2.6% ± 0.2% cells per hour (monitored in the lateral epidermis between 15 and 22.5 hr APF; n = 4 pupae; Figures 3C and 3D). Conversely, overexpression of either Tkv^{DN} or a TkvRNAi transgene yielded only a few marked LECs that delaminated precociously at an average rate of 13% per hour (n = 4 pupae each). The low number of mutant LECs per animal rendered in these latter conditions precluded further detailed statistical analysis. Together, these data suggest that the autocrine function of Dpp signaling in LECs could be to limit their delamination rate, eventually preventing precocious elimination. Remarkably, LEC delamination rates were not affected by clonal autonomous Dad overexpression, which should only upset transcriptional events downstream of Mad (6.6% ± 1.3% for Dad-overexpressing LECs and 6.8% ± 0.5% cells per hour for sibling WT LECs; n = 5 pupae).

Dpp-Dependent Cellular Mechanisms Regulating Histoblast Invasive Behavior

Transforming growth factor-β (TGF-β) function in motility and invasiveness in cultured cells and metastatic tumors is linked to a coordinated sequence of disassembly of cell junctions, cytoskeletal reorganization, loss of polarity, and remodeling of cell-matrix adhesions [5]. Likewise, histoblast expansion is associated with a reduction of cell-cell contacts and cell-substrate and cytoskeleton remodeling (Figure 1). To test whether Dpp signaling is required to modulate cell adhesion or cytoskeleton dynamics, we cell-autonomously interfered with Dpp activation in histoblasts and analyzed components involved in these processes.

In contrast to wild-type, leading *tkv* histoblasts from clones induced before the onset of expansion failed to emit cellular protrusions and change shapes (Figure 4A). This phenotype is equivalent to that observed after interfering with actin dynamics [4]. Accordingly, filamentous actin was autonomously depleted from the cellular apical domains in clones unable to respond to Dpp (UAS-Dad clones) (Figure 4B). In contrast, abundant apical short actin-rich membrane protrusions were observed in clones of cells expressing the Tkv^{QD} receptor (Figure 4C). Together, these findings show that Dpp signaling autonomously modulates actin dynamics, which itself is pivotal for histoblast invasiveness.

During nest expansion, leading histoblasts located at the periphery show a characteristic flattening associated with low density at the cell membrane of adhesion molecules such as DE-cadherin and Discs large (Figure 1 and data not shown). In fact, fluorescence recovery after photobleaching (FRAP) analyses showed that DE-cadherin turnover (rate of fluorescence recovery $-\ \tau_{1/2}$) was significantly faster ($p < 0.001$) in histoblasts at the periphery ($\tau_{1/2} = 42.29$ s) than at the center ($\tau_{1/2} = 88.01$ s). The DE-cadherin mobile fraction (A), however, did not change (0.698 at the periphery and 0.734 at the center) (Figure 4D). In addition, we found that histoblasts unable to respond to Dpp (Dad-expressing clones) at the nest periphery showed a very much compacted morphology and higher density of Discs large and β-catenin than neighbors (Figure 4E and data not shown). To test the possibility that the decrease of DE-cadherin packing at the periphery could be functionally significant for cell invasiveness, we clonally overexpressed a functional DE-cadherin-GFP fusion. Remarkably, DE-cadherin-expressing clones, like Dpp signaling loss-of-function clones, were largely excluded from the expanding front by 22–26 hr APF (with less than 40% of the clones [n = 26] abutting the nest edge) and remained in the center of the nest (Figure 4F). Jointly, these observations show that the decrease of cell adhesion component density at the periphery of nests (potentially reducing cell-cell contact strength) is under Dpp control and suggest that this attenuation allows histoblasts to become more plastic and motile.

At the onset of nest expansion, peripheral histoblasts remodel β-integrin localization and detach from the ECM, which is being degraded (Figure 1). To determine whether Dpp controls histoblast-substrate adhesion, we interfered with Dpp signaling in histoblasts by clonal expression of Dad or Tkv^{QD}. Noticeably, a reduction in Dpp signaling caused a failure in the remodeling of β-integrin, which became abnormally clumped on the lateral and basal surface of histoblasts (Figure 4G). In contrast, constitutive activation of Dpp signaling resulted in the almost absolute exclusion of β-integrin from basal domains, both at the periphery and at the nest center (Figure 4H). Whether these shifts in the intracellular localization of β-integrin are necessary for modulating histoblast motility remains to be determined.

Discussion

dpp encodes a secreted polypeptide of the TGF-β superfamily [11], which acts as a secreted autocrine and paracrine morphogen regulating growth, patterning, and epithelial organization [12–16] and controlling epithelial movements [17, 18]. We have found that Dpp secreted from LECs leads to paracrine-graded activation of its signaling pathway at the periphery of histoblast nests during expansion. Across these nests, Dpp activity confers differential cellular plasticity and motility: cells with the highest activity behave as leaders and intercalate between surrounding LECs, whereas cells that did not activate the pathway remain passive and immotile (Figure 3E). Dpp signaling activation in histoblasts is implemented at the transcriptional level by Mad, probably hitting several effectors simultaneously, and produces a complex, multifaceted phenotype. Mechanistically, at the cellular level, Dpp signaling enforces a reduction of DE-cadherin (and other adhesion molecules) density in the membrane of peripheral histoblasts, which correlates with an increase in DE-cadherin turnover and the relaxation of cell-cell contacts. Indeed, overexpression of DE-cadherin led to a phenotype similar to Dpp signaling loss-of-function conditions. Furthermore, Dpp signaling also intensifies actin cytoskeleton dynamics, which is instrumental for leading histoblast invasiveness [4].

The function of Dpp signaling in histoblasts is similar to that observed in cell flattening in imaginal discs [19], the regulation of migration of peripheral glia [20], the extension of tracheal branches [21, 22], and cell shape changes during dorsal closure [23]. However, Dpp signaling does not mediate cell invasiveness in any of these cases. On the other hand, the autocrine role of Dpp signaling in LECs, which appears to prevent their precocious delamination, is mechanistically different and does not involve Mad-mediated activation of *dad* expression.

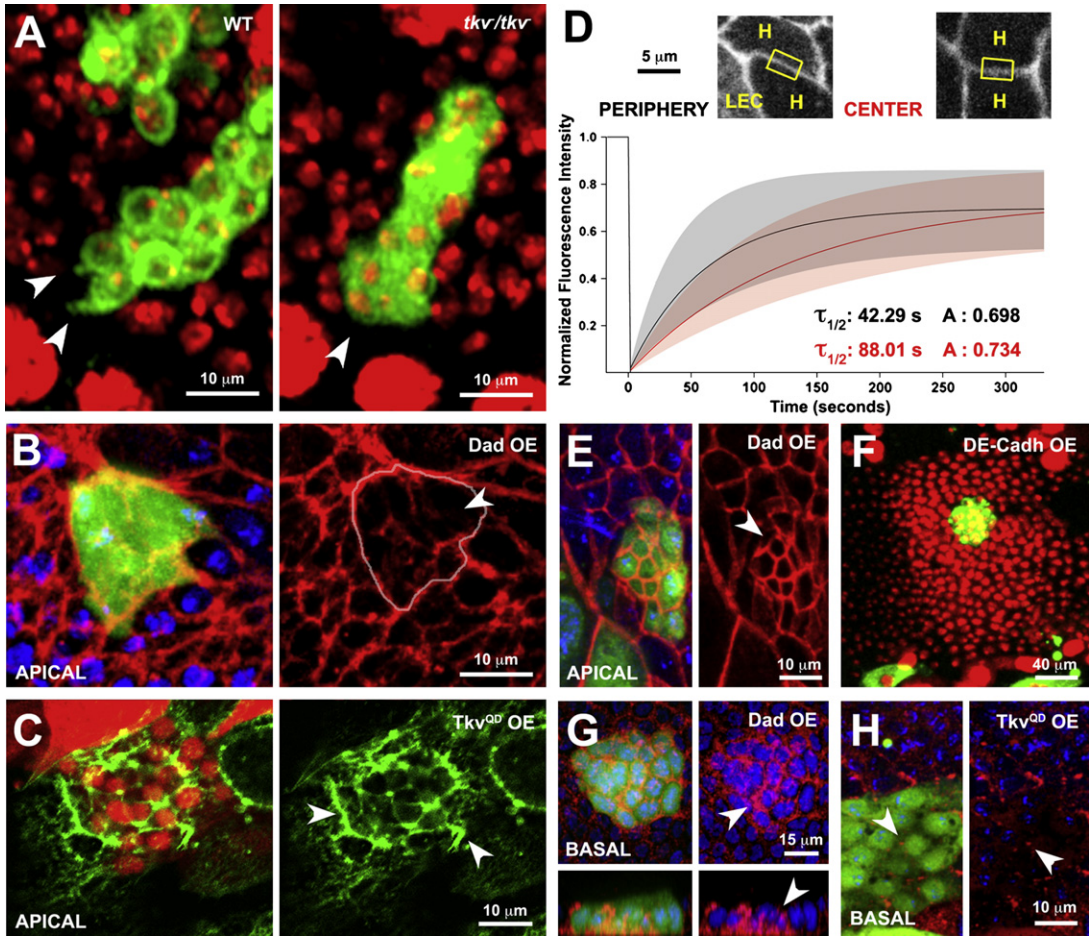

Figure 4. Dpp Promotes Cellular Motility by Modulating Actin Dynamics, Cell-Cell Contacts, and Cell Substrate Adhesion

(A) Left: WT MARCM clone in the posterior dorsal nest at 18 hr APF. Arrowheads point to invasive cellular protrusions at the tip of leading cells. Right: *tkv* homozygous MARCM clone in the anterior dorsal nest at 18 hr APF. The cells from the clone are more condensed than WT neighbors, and the leading cells are blunt and lack cellular protrusions (arrowhead).

(B) Projection of the apical sections of a UAS-Dad-overexpressing clone (green) stained with phalloidin (red) showing a general downregulation of the actin cytoskeleton. Arrowhead points to remnants of actin filaments in the apical surface of mutant cells.

(C) Projection spanning the apical surface of a UAS-Tkv^{QD} clone (red) stained with phalloidin (green) showing abundant apical actin-rich protrusions and extensions (arrowheads).

(D) Fluorescence recovery after photobleaching (FRAP) experiments were performed on DE-cadherin-GFP-expressing pupae at 18 hr APF. For each FRAP experiment, three apical focal planes were recorded (n = 21 for central and n = 18 for peripheral histoblasts). Integrated density (ID) of fluorescence was measured over time for each region of interest. The black curve plots the normalized exponential recovery for peripheral cells (according to Equation 1 in Supplemental Experimental Procedures), with average values $\tau_{1/2}$ = 42.29 s and mobile fraction A = 0.698, issued from n = 18 curve fits of FRAP sequences. The gray shaded area delimits the range of variation described by the standard deviations of the distributions of $\tau_{1/2}$ and A (n = 18), i.e., the upper limit is calculated with $\tau_{1/2}$ = 42.29 + 4.09 s (average + Δ) and A = 0.698 + 0.0395 (average + Δ), and the lower limit is calculated with $\tau_{1/2}$ = 42.29 − 4.09 s and A = 0.698 − 0.0395. The red curve shows the same plots for the central cells with average value of $\tau_{1/2}$ = 88.01 s with Δ ± 6.05 s and A = 0.734 with Δ ± 0.0305, issued from n = 21 curve fits of FRAP sequences. The pink shaded area delimits the range of variation described by the standard deviations of the distributions of $\tau_{1/2}$ and A (n = 21) for central histoblasts. Note that mobile fraction A is similar for both cell types, whereas the dynamic recoveries described by $\tau_{1/2}$ show significant differences.

(E) UAS-Dad clone (green) stained for Dlg (red) and captured in the periphery during nest expansion. The cells from the clone show extreme constriction and display high Dlg signal density in contrast to adjacent WT peripheral histoblasts. The apical area of Dad-expressing cells adjacent to the periphery drops by 61.2% (n = 17 from three different clones, 20 hr APF) when compared to WT peripheral cells (n = 30). Circularity of these cells increases, however, by 27.9%. Discs large levels were equivalent in Dad-expressing cells and WT peripheral neighbors (627.24 ± 87.81 ID units per cell), but its density increased from 10.42 ± 0.80 to 18.33 ± 0.74 ID units per perimeter unit. These parameters were very similar to those determined for WT histoblasts at the center of the nests (609.48 ± 57.42 ID units per cell and 17.17 ± 0.93 ID units per perimeter unit [n = 28]).

(F) Functional UAS-DE-cadherin-GFP-overexpressing clones generated in the blastoderm via the MARCM system. In expanding histoblast nests (24 hr APF), UAS-DE-cadherin-GFP clones (green) sort toward the center of the nest and are unable to contribute to the invasion of the larval epithelia.

(G) UAS-Dad clones (green) stained for β-integrin (red). The basal surfaces of cells from the clone show clumping of β-integrin (arrowhead). The bottom panels present a transverse 3D reconstruction revealing enrichment of basolateral β-integrin in mutant cells.

(H) UAS-Tkv^{QD} clones (green) stained with anti β-integrin (red). The basal surfaces of cells from the clone (green) show redistribution of β-integrin from the basolateral surface to ectopic puncta (arrowhead).

Nuclei were labeled in blue (B, E, G, and H) or red (A and F) with DAPI.

This function may participate in the coordination of LECs' death with the progression of histoblast expansion.

Interestingly, histoblast locomotion appears to progress quite differently from other known epithelial cell migratory events. The degradation of the basal lamina precedes the spreading of histoblasts, which attach apically to the overlaying chitinous pupal cuticle. These attachments resemble those of the spiral limbus and the organ of Corti to the tectorial membrane in mammals' inner ear [24] or those found during embryonic implantation and leukocyte transendothelial migration [25], where endometrium and endothelium apical surfaces serve as anchoring sites for blastocysts or leukocytes. Strikingly, the ZP protein Piopio, which shares a zona pellucida domain with mammalian primary components of the inner layer of the apical ECM [26], including α-tectorin [24], is apically expressed by histoblasts and LECs (data not shown). Whether Piopio might act as an anchor to the pupal cuticle remains to be determined.

In contrast to the limited consequences of the migratory behavior of single cells, collective cell migration results in profound changes in tissue morphogenesis [1, 27]. Furthermore, multicellular invasion contributes to cancer spreading [28, 29]—e.g., the invasive edges of fibrosarcomas and ductal breast carcinomas commonly develop into multicellular strands [6]. Notably, the response to TGF-β family ligands contributing to metastatic carcinoma cell motility is phenotypically characterized by the downregulation of epithelial markers at the transcriptional and/or posttranslational levels and by the reorganization of the actin cytoskeleton. TGF-β also acts as an important modulator of tumor microenvironment and activates the expression of metalloproteases and the degradation of the basal lamina [30, 31]. The invasive behavior of leading histoblasts controlled by Dpp signaling in *Drosophila* constitutes an important developmental model of collective migration where, through the combination of advanced live microscopy and clonal genetic interference, the mechanisms controlling active motility and invasiveness can be studied in vivo.

Supplemental Information

Supplemental Information includes Supplemental Experimental Procedures, three figures, and five movies and can be found with this article online at doi:10.1016/j.cub.2010.01.063.

Acknowledgments

We would like to thank all members of our laboratories for encouragement and criticism and C. Bakal, K. Basler, B. Belo, F. Bejarano, J. Colombelli, H. Herranz, and E. Rebollo for reagents and advice. We thank the Vienna Drosophila RNAi Center, the Bloomington Stock Center, and the Transgenic RNAi Resource Project at Harvard Medical School (NIH/NIGMS R01-GM084947) for providing fly stocks used in this study. N.N. held a Formación de Profesorado Universitario PhD studentship, C.P.-R. held a "La Caixa" master fellowship, and S.M.-C. is supported by a PhD fellowship from the Fundação para a Ciência e a Tecnologia (Portugal). N.N. would like to thank U. Tepass for his assistance and support. Research in E.M.-B.'s laboratory is funded by grants from the Spanish Ministry of Science and the European Union. Research in M.A.'s laboratory is supported by the Swiss National Science Foundation, Kanton Basel-Stadt, Kanton Basel-Landschaft, and the European Union.

Received: August 23, 2009
Revised: January 12, 2010
Accepted: January 14, 2010
Published online: March 11, 2010

References

1. Friedl, P., Hegerfeldt, Y., and Tusch, M. (2004). Collective cell migration in morphogenesis and cancer. Int. J. Dev. Biol. *48*, 441–449.
2. Friedl, P., and Wolf, K. (2003). Tumour-cell invasion and migration: Diversity and escape mechanisms. Nat. Rev. Cancer *3*, 362–374.
3. Madhavan, M.M., and Madhavan, K. (1980). Morphogenesis of the epidermis of adult abdomen of Drosophila. J. Embryol. Exp. Morphol. *60*, 1–31.
4. Ninov, N., Chiarelli, D.A., and Martín-Blanco, E. (2007). Extrinsic and intrinsic mechanisms directing epithelial cell sheet replacement during Drosophila metamorphosis. Development *134*, 367–379.
5. Zavadil, J., and Böttinger, E.P. (2005). TGF-beta and epithelial-to-mesenchymal transitions. Oncogene *24*, 5764–5774.
6. Christiansen, J.J., and Rajasekaran, A.K. (2006). Reassessing epithelial to mesenchymal transition as a prerequisite for carcinoma invasion and metastasis. Cancer Res. *66*, 8319–8326.
7. Ninov, N., Manjón, C., and Martín-Blanco, E. (2009). Dynamic control of cell cycle and growth coupling by ecdysone, EGFR, and PI3K signaling in Drosophila histoblasts. PLoS Biol. *7*, e1000079.
8. Massagué, J., Seoane, J., and Wotton, D. (2005). Smad transcription factors. Genes Dev. *19*, 2783–2810.
9. Kopp, A., Blackman, R.K., and Duncan, I. (1999). Wingless, decapentaplegic and EGF receptor signaling pathways interact to specify dorsoventral pattern in the adult abdomen of Drosophila. Development *126*, 3495–3507.
10. Weiss, A., Charbonnier, E., Ellertsdóttir, E., Tsirigos, A., Wolf, C., Schuh, R., Pyrowolakis, G., and Affolter, M. (2010). A conserved activation element in BMP signaling during Drosophila development. Nat. Struct. Mol. Biol. *17*, 69–76.
11. Affolter, M., and Basler, K. (2007). The Decapentaplegic morphogen gradient: From pattern formation to growth regulation. Nat. Rev. Genet. *8*, 663–674.
12. Greenwood, S., and Struhl, G. (1999). Progression of the morphogenetic furrow in the Drosophila eye: The roles of Hedgehog, Decapentaplegic and the Raf pathway. Development *126*, 5795–5808.
13. Morata, G., and Sánchez-Herrero, E. (1999). Patterning mechanisms in the body trunk and the appendages of Drosophila. Development *126*, 2823–2828.
14. Ribeiro, C., Neumann, M., and Affolter, M. (2004). Genetic control of cell intercalation during tracheal morphogenesis in Drosophila. Curr. Biol. *14*, 2197–2207.
15. Gibson, M.C., and Perrimon, N. (2005). Extrusion and death of DPP/BMP-compromised epithelial cells in the developing Drosophila wing. Science *307*, 1785–1789.
16. Shen, J., and Dahmann, C. (2005). Extrusion of cells with inappropriate Dpp signaling from Drosophila wing disc epithelia. Science *307*, 1789–1790.
17. Martin-Blanco, E., Pastor-Pareja, J.C., and Garcia-Bellido, A. (2000). JNK and decapentaplegic signaling control adhesiveness and cytoskeleton dynamics during thorax closure in Drosophila. Proc. Natl. Acad. Sci. USA *97*, 7888–7893.
18. Martín-Blanco, E., and Knust, E. (2001). Epithelial morphogenesis: Filopodia at work. Curr. Biol. *11*, R28–R31.
19. McClure, K.D., and Schubiger, G. (2005). Developmental analysis and squamous morphogenesis of the peripodial epithelium in Drosophila imaginal discs. Development *132*, 5033–5042.
20. Yoshida, S., Soustelle, L., Giangrande, A., Umetsu, D., Murakami, S., Yasugi, T., Awasaki, T., Ito, K., Sato, M., and Tabata, T. (2005). DPP signaling controls development of the lamina glia required for retinal axon targeting in the visual system of Drosophila. Development *132*, 4587–4598.
21. Kato, K., Chihara, T., and Hayashi, S. (2004). Hedgehog and Decapentaplegic instruct polarized growth of cell extensions in the Drosophila trachea. Development *131*, 5253–5261.
22. Ribeiro, C., Ebner, A., and Affolter, M. (2002). In vivo imaging reveals different cellular functions for FGF and Dpp signaling in tracheal branching morphogenesis. Dev. Cell *2*, 677–683.
23. Fernández, B.G., Arias, A.M., and Jacinto, A. (2007). Dpp signalling orchestrates dorsal closure by regulating cell shape changes both in the amnioserosa and in the epidermis. Mech. Dev. *124*, 884–897.
24. Legan, P.K., Lukashkina, V.A., Goodyear, R.J., Kössi, M., Russell, I.J., and Richardson, G.P. (2000). A targeted deletion in alpha-tectorin

reveals that the tectorial membrane is required for the gain and timing of cochlear feedback. Neuron *28*, 273–285.

25. Dominguez, F., Yáñez-Mó, M., Sanchez-Madrid, F., and Simón, C. (2005). Embryonic implantation and leukocyte transendothelial migration: Different processes with similar players? FASEB J. *19*, 1056–1060.
26. Bökel, C., Prokop, A., and Brown, N.H. (2005). Papillote and Piopio: Drosophila ZP-domain proteins required for cell adhesion to the apical extracellular matrix and microtubule organization. J. Cell Sci. *118*, 633–642.
27. Farooqui, R., and Fenteany, G. (2005). Multiple rows of cells behind an epithelial wound edge extend cryptic lamellipodia to collectively drive cell-sheet movement. J. Cell Sci. *118*, 51–63.
28. Nabeshima, K., Inoue, T., Shimao, Y., Okada, Y., Itoh, Y., Seiki, M., and Koono, M. (2000). Front-cell-specific expression of membrane-type 1 matrix metalloproteinase and gelatinase A during cohort migration of colon carcinoma cells induced by hepatocyte growth factor/scatter factor. Cancer Res. *60*, 3364–3369.
29. Hegerfeldt, Y., Tusch, M., Bröcker, E.B., and Friedl, P. (2002). Collective cell movement in primary melanoma explants: Plasticity of cell-cell interaction, beta1-integrin function, and migration strategies. Cancer Res. *62*, 2125–2130.
30. Wolf, K., Wu, Y.I., Liu, Y., Geiger, J., Tam, E., Overall, C., Stack, M.S., and Friedl, P. (2007). Multi-step pericellular proteolysis controls the transition from individual to collective cancer cell invasion. Nat. Cell Biol. *9*, 893–904.
31. Gupta, G.P., and Massagué, J. (2006). Cancer metastasis: Building a framework. Cell *127*, 679–695.